

Unusual coelom formation in the direct-type developing sand dollar *Peronella japonica*

メタデータ	言語: eng 出版者: 公開日: 2017-10-03 キーワード (Ja): キーワード (En): 作成者: メールアドレス: 所属:
URL	http://hdl.handle.net/2297/29459

Unusual coelom formation in the direct-type developing sand dollar *Peronella japonica*

Jun Tsuchimoto, Toshihiro Yamada, and Masaaki Yamaguchi*

Division of Life Science, Graduate School of Natural Science and Technology, Kanazawa University,

Kakuma, Kanazawa 920-1192, Japan

***Author for correspondence**

Masaaki Yamaguchi

Division of Life Science, Graduate School of Natural Science and Technology, Kanazawa University,

Kakuma, Kanazawa, Ishikawa 920-1192, Japan

Tel: +81-76-264-6233

Fax: +81-76-264-6215

E-mail: myama@kenroku.kanazawa-u.ac.jp

Running Title: Unusual coelom formation in *Peronella japonica*

Keywords: Echinoderm; Echinoid; Coelom; Hydrocoel; Enterocoely; Schizocoely

Grant Sponsor: JSPS KAKENHI

Grant Number: DC2-22-2510

Grant Sponsor: JSPS KAKENHI

Grant Number: 21570222

ABSTRACT

Peronella japonica is a sand dollar with a zygote that develops into an abbreviated pluteus but then metamorphoses on day three. The adult rudiment formation is unique; it uses a median position of the hydrocoel and a stomodeum-like invagination of vestibule that covers the dorsal side of the hydrocoel. However, the developmental processes underlying coelom formation remains unclear. In this study, we examined this process by reconstructing three-dimensional images from serial sections of larvae. We show that the left coelom developed by both schizocoely and enterocoely from the archenteron tip, whereas the hydrocoel and right coelom formed by enterocoely from the archenteron. This coelom formation arranged the coelomic compartments directly along the adult oral-aboral axis by skipping the initial bilateral phases. Furthermore, our data indicate *P. japonica* retains ancestral asymmetry along the left-right axis in the location of the adult rudiment.

INTRODUCTION

In echinoids, most species adopt one of two developmental modes. Indirect developers make numerous small eggs, which develop into larvae that require a feeding period before metamorphosis. In contrast, direct developers make few large eggs. These large eggs then develop into larvae that do not feed, reducing the time in the water column before metamorphosis (Emllet et al., 1987; Raff, 1987). Indirect development via a planktotrophic pluteus larva is thought to be the ancestral mode of echinoid development, and direct development with a non-feeding lecithorophic larva is thought to have evolved independently in several lineages (Strathmann, 1978; Raff, 1987; Emllet, 1990).

Peronella japonica is a direct-type developing sand dollar, first characterized by Mortensen (1921). Its eggs are ~300 μm in diameter, making them the smallest known among direct-developing echinoids (Okazaki and Dan, 1954; Wray and Raff, 1991). The larva may also represent an intermediate form in the evolution from indirect to typical direct development (Raff, 1987; Amemiya and Arakawa, 1996; Yajima, 2007; Iijima et al., 2009). Indeed, the zygote forms micromeres at the 16-cell stage (Fig. 1A), and the descendants ingress into the blastocoel as the primary mesenchyme cells (PMCs) before hatching (Fig. 1B) to eventually differentiate to skeletogenic cells (Okazaki, 1975; Amemiya and Arakawa, 1996; Yajima, 2007; Iijima et al., 2009). The embryo develops into an abbreviated pluteus larva

with a pair of the postoral arms (Fig. 1E) and then metamorphoses without feeding on day three (Fig. 1F; Okazaki and Dan, 1954; Okazaki, 1975). PMCs contribute exclusively to the formation of larval skeletal elements, whereas late mesenchyme cells, similar to the secondary mesenchyme cells (SMCs) of typical indirect developers, are involved in adult skeletogenesis (Yajima, 2007; Iijima et al., 2009).

P. japonica exhibits unique adult rudiment formation (Mortensen, 1921; Okazaki and Dan, 1954; Okazaki, 1975). Gastrular invagination begins with the migration of late mesenchyme cells (Fig. 1C). Within a few hours, another invagination begins in the ectoderm in the center of the flattened oral field, eventually developing into a stomodeum-like invagination (Fig. 1D, G). This invagination extends along the dorsal side of the endomesoderm to the posterior end of the larva, forming the vestibule (Fig. 1E, H, I). The mouth does not open, and the blastopore closes, resulting in a blind sac (Fig. 1G). At ~24 h, the hydrocoel begins to differentiate in a nearly median position from the left or right coelom, whichever lies close to the ventral side of the larva (Okazaki and Dan, 1954; Fig. 1H, I). The location of the hydrocoel, together with the unusual median position of the vestibule, is strikingly different from the corresponding structures in other echinoids. However, the processes underlying formation of coelomic compartments, particularly the origin of the hydrocoel, remain undefined. After the enlargement of the hydrocoel, five lobes are pushed out and arranged in a bilaterally symmetrical fashion with regard to the

midline of the larva. Metamorphosis then begins with the protrusion of rudimentary spines and tube feet from the dorsal side of the larva (Okazaki and Dan, 1954; Okazaki, 1975).

In this study, we examined the formation of coelomic compartments which are enclosed by the water vascular system or which become the main body cavities in *P. japonica*. To do this, we reconstructed three-dimensional (3D) images from serial sections of larvae. We show that the left coelom developed by both schizocoely and enterocoely from the archenteron tip. In contrast, the hydrocoel and right coelom sequentially formed from the archenteron by enterocoely. Furthermore, we defined each ambulacrum of *P. japonica* according to Lovén's system by raising juveniles until they had a mouth and anus.

RESULTS

***P. japonica* formed an adult anus at the anterior end of the larva**

Similarly to Okazaki and Dan (1954; Fig. 1G), we defined the site of the vestibular opening (stomodeum-like structure in typical indirect developers) as the anterior side of the larva. We define the ventral side as the side containing the blastopore. The blastopore closes during the prism stage but remains as a pit for several hours. The vestibule, therefore, invaginates along the dorsal side of the larva

along the anteroposterior (AP) axis (Fig. 1H, I).

Fig. 2 shows a *P. japonica* imago three weeks after metamorphosis, which had been fed the diatom *Chaetoceros gracilis*. It developed five sets of dental elements, adult six-rayed spines, and 15 tube feet (out of focus in this photo). It also retained two larval postoral rods (black and white arrowheads in Fig. 2), which are traces of the anterior side of the larva. In our culture condition, several percent of the imagoes (n_>100) retained the larval rods. We observed the digestive tract by diatom chlorophyll fluorescence and found that it started at the masticatory apparatus in the oral center of the imago, ~~enrolled~~involved counter-clockwise (when viewed from the aboral side) approximately three quarters around, reached the former anterior side of the larva and twisted nearly once around, and ended at the anus (red arrowhead in Fig. 2) between the postoral rods. This means that the AP axes of the larva and juvenile are parallel but opposite in direction. Lovén (1874) developed a numbering system for the ambulacra of echinoids based on the AP axis of Irregularia species. According to Lovén's system, we defined each ambulacrum of *P. japonica* (see below).

The left coelom developed by both schizocoely and enterocoely from the archenteron tip

To examine the formation of the coeloms in *P. japonica* larvae, we reconstructed 3D images from serial sections of larvae (2.5–3 μm thick) using DeltaViewer.

We examined gastrulae at 16 h which had developed the vestibule in the oral field (Fig. 3A), and found that the archenteron leaned toward the left side. We also observed a number of mesenchyme cells, similar to the SMCs of indirect developers, migrating out of the archenteron tip (Fig. 3B). Fig. 4A–D shows four of 70 horizontal serial sections (3 μm thick) along the dorsoventral (DV) axis of an early prism larva at 18 h, in which the ectodermal layer, a mass of mesenchyme cells, and archenteron-derived epithelia are colored green, red, and yellow, respectively. In the coloring process, we have eliminated the mesenchyme cells scattered in the blastocoel, including the PMCs and the blastocoelar cells. Fig. 4E and Fig. 4F–H indicate reconstructed 3D images of the exterior and internal endomesodermal structures viewed from the right-posterior and slightly dorsal side of the larva, respectively. The exterior image (Fig. 4E) is shown in a reduced scale compared to the internal structures (Fig. 4F–H). From the archenteron, a coelomic pouch, marked in yellow, elongated counter-clockwise to the anterior and then dorsal direction; the tip of coelomic pouch reached the anterodorsal side of the larva, which was adjacent to the vestibular floor (arrowheads in Fig. 4D, G, H). The mesenchyme, marked in red, covered the left side of the coelomic pouch (Fig. 4A–D, G). We should note that the boundary between

the mesenchyme and enterocoelic epithelia was obscured in portions just below the tip of the coelomic pouch (blue asterisks in Fig. 4C, G, H; arrowheads in Fig. S1). This lobe, marked in yellow, appeared to participate in the formation of the left coelom probably by enterocoely since it disappeared from the enterocoelic epithelium by the next stage, and the portion of the left coelomic cavity was encircled by an epithelial layer in the next stage (Fig. 5; arrowheads in Fig. S2).

Fig. 5 shows six of 84 horizontal serial sections (3 μm thick) of an early pluteus larva at 24 h, and Fig. 6 shows reconstructed 3D images of the exterior and internal endomesoderm structures, viewed from the right-posterior or left-anterior side of the larva, both with a slightly dorsal view. Color code is the same as in Fig. 4, except for red. Red shows the left coelom developed from the mesenchyme plus an epithelial lobe formally marked in yellow (asterisks in Fig. 4). By this stage, the mesenchyme and lobe completely separated from the enterocoelic epithelium and started to form coelomic cavities (Fig. 5; Fig. S2). Additionally, the coelom expanded to the anterior side of the larva on either side of the enterocoelic structure. The left side of the coelom extended ventrally while the right side extended dorsally (Fig. 5B–F; Fig. 6C, G). Together with the original left side location, the C-shaped coelom dominantly covered the enterocoelic structures on the left side, with a ventral tilt of the left side (Fig. 6C, G).

The hydrocoel and right coelom sequentially developed by enterocoely from the archenteron

In an early prism larva at 18 h, the tip of the coelomic pouch reached the anterodorsal side of the larva (arrowheads in Fig. 4), forming the putative right coelom. During the next six hours of hydrocoel formation, the tip of the coelomic pouch elongated in the posterior direction until nearly reaching the dorsal center of the larva. At the end of elongation, the newly formed hydrocoel was inserted into the C-shaped putative left coelom (Fig. 5F; Fig. 6C, G). The putative right coelom corresponded to a turning portion of the coelomic pouch, from the anterior to the dorsal direction (Fig. 5D–E; Fig. 6D, H). This portion of the coelomic pouch became coelom-like in shape with a relatively large cavity in the pluteus larva at 28 h (Fig. 7B, C; Fig. 8D).

The hydrocoel, left somatocoel, and right somatocoel were arranged along the DV axis of the larva

Fig. 7 shows six of 65 horizontal serial sections (2.5 μm thick) of a pluteus larva at 28 h that were used to reconstruct the 3D images of the exterior and internal structures (Fig. 8). Color code is the same as in Fig. 5. By the pluteus larva stage, the formerly C-shaped left coelom had fused at the anterior side of the larva to encircle the hydrocoel (Fig. 8F, G). The hydrocoel started branching lobes to form the podium primordia. According to Lovén's system, we defined the presumptive ambulacra I–V, although the

branches of the hydrocoel in ambulacra I and V were immature compared to those in ambulacra II, III, and IV (Fig. 8D, H). *P. japonica* juveniles have a triad of podia in each ambulacrum after metamorphosis (Okazaki and Dan, 1954). At 28 h, the primordia of a triad of podia and the radial canal developed exclusively in the ambulacrum III (blue asterisks and ra, respectively, in Fig. 8D, H) on the future anterior side of adult sand dollars. On the other hand, the left coelom generated projections against the vestibular floor that covered the dorsal side of the hydrocoel and left coelom (Fig. 8B, F). This projection was evident in presumptive interambulacra 2 and 3 (Fig. 8C, G). We believe that these projections are rudiments of the dental sac because their development is similar to the formation of dental sacs from the left somatocoel in indirect developers (MacBride, 1903; von Übish, 1913; Smith et al., 2008).

Fig. 9 shows six of 71 horizontal serial sections (2.5 µm thick) of a pluteus larva at 32 h that were used to reconstruct the 3D images of the exterior and internal structures viewed from either the dorsal side or the right-posterior (and slightly dorsal) side of the larva (Fig. 10). Color code is the same as in Fig. 5. By 32 h, the five lobes of the hydrocoel were evident, although closure of the hydrocoel crescent resulting in a closed ring canal had not yet occurred between ambulacra IV and V (arrow in Fig. 10D). This is consistent with what is observed in echinoids (Hotchkiss, 1995). Although the primary lobe was largely bilateral along Lovén's axis that passes through both the ambulacrum III and the

interambulacrum 5 (ra3–ds5 in Fig. 10C), it did not lie on the midline of the larva, but on the left side (see location of the future ring canal; arrow in Fig. 10D). Along with the location, the left coelom tilted leftward (see positions of dental sacs in Fig. 10B, F). By this stage, five dental sacs developed from the left coelom and interdigitated with five lobes of the hydrocoel (ds1–5 in Fig. 10C, G). This observation indicates that dental sacs in the posterior side of the larva (ds2, 3 in Fig. 8B, F) developed before the anterior ones, and suggests that the left coelom should actually be designated the left somatocoel, like that found in the larval anatomy of indirect developers (Smith et al., 2008).

At the same developmental time point, the right coelom, which had been largely segregated from the enteric sac (Fig. 9A–E), narrowed in the anterodorsal portion (arrow in Fig. 9D) and divided the coelom into anterodorsal and posteroventral sacs. The anterodorsal sac was connected to the hydrocoel at the base of the presumptive ambulacrum II via an epithelial duct (arrowhead in Fig. 9E; st in Fig. 10H).

Although further analysis is required for definitive identification, we believe the duct is a presumptive stone canal. In indirect-developing echinoids, the stone canal that is associated with the left axocoel (ampulla) and the hydroporic canal connects the ring canal to the madreporite on genital plate 2 (MacBride, 1903; Gordon, 1929; Smith et al., 2008). This presumptive stone canal suggests that the anterodorsal and posteroventral sacs derived from the right coelom may be the axocoel and right

somatocoel, respectively. This classification is consistent with coelomic stacking, the echinoderm-characteristic arrangement of coeloms where the hydrocoel, left somatocoel, and right somatocoel are stacked along the oral-aboral axis of adults (David and Mooi, 1998; Peterson et al., 2000). Our data show that the hydrocoel, left somatocoel, and putative right somatocoel were arranged along the DV axis of the larva with a leftward tilt in *P. japonica* (Fig. 9, 10).

DISCUSSION

Unusual coelom formation in *P. japonica*

Our observations indicate that *P. japonica* development represents an example of an extremely modified coelom formation in echinoids. The left coelom developed from mesenchyme cells that had migrated out of the archenteron tip and an epithelial lobe that had projected from the archenteron, whereas the hydrocoel and right coelom sequentially formed from the archenteron by enterocoely (Fig. 4, 5, S1, S2).

Although enterocoely is the typical coelom formation strategy employed in most echinoderms, schizocoely has been described in several direct-developing species, including the spatangoid *Abatus cordatus* (Schatt and Féral, 1996), the ophiuroid *Amphipholis squamata* (Fell, 1946), and the crinoid *Oxycomanthus japonica* (Kubota, 1988).

The coelom formation of *P. japonica* is unique in two regards. The first is that *P. japonica* uses two means of coelom formation: both schizocoely and enterocoely for the left somatocoel, and enterocoely for formation of the rest of coelomic compartments, including the hydrocoel, stone canal, axocoel, and right somatocoel. The second unique feature is that *P. japonica* uses sequential coelom formation from the archenteron tip. In indirect developers, the left and right coelomic pouches pinch off from the respective sides of the archenteron near the end of gastrulation. Then, during the eight-arm pluteus stage, each coelom divides into three compartments, the axocoel, hydrocoel, and somatocoel, along either side of the esophagus and stomach (Smith et al., 2008). Even in the direct developers *Asthenosoma iijimai* and *Heliocidaris erythrogramma*, the left and right coeloms form independently from the archenteron tip, and then the left coelom divides into the hydrocoel and left somatocoel (Amemiya and Emler, 1992; Ferkowicz and Raff, 2001). Thus, unlike both the indirect and the direct developers, the *P. japonica* archenteron tip sequentially generates coelomic compartments: first, mesenchyme cells plus an epithelial lobe that give rise to the future left somatocoel, and then the future hydrocoel, axocoel, and right somatocoel by enterocoely. By skipping the initial bilateral phases of the coelom formation, sequential coelom formation results in direct arrangement of the coelomic compartments along the adult oral-aboral axis in both stacking order and connection via the stone canal.

Additionally, *P. japonica* probably skips formation of the hydroporic canal and hydropore. In indirect developers, these structures develop from the left coelom prior to its differentiation into the left axocoel, hydrocoel, and somatocoel (Smith et al., 2008). However, we did not observe these types of tubular structures or an opening in either the serial sections or the 3D images of *P. japonica* larvae from the early prism (18 h) to pluteus larva (32 h) stages. In fact, the dorsal and ventrolateral sides of the endomesoderm were covered with the vestibular floor consisting of stratified epithelia and a gap-less larval ectodermal layer with a blastopore, respectively.

P. japonica does not form larval mouth (stomodeum), but instead develops a vestibule in the region (Okazaki and Dan, 1954; Kitazawa and Amemiya, 1997). In addition to the direct arrangement of coelomic compartments along the adult oral-aboral axis, this precocious formation of the vestibule may contribute to the rapid adult rudiment formation in *P. japonica*.

***P. japonica* retains traits of indirect-developing sand dollars**

Unlike in Echinacea species (so-called regular urchins; Smith, 1984), the bilateral symmetry of adult skeletal elements in *Echinarachnius parma*, an indirect-developing sand dollar, is marked along Lovén's axis rather than von Übisch's axis (Gordon, 1929). Furthermore, Gordon (1929) showed *E.*

parma-characteristic features; the ambulacrum III develops more rapidly than the others, and the skeletal plates in interambulacra 2 and 3 are larger and more numerous than those in the three posterior areas of adults. In *P. japonica*, we observed bilateral symmetry of the primary lobe along Lovén's axis (Fig. 8, 10) and precocious formation of both the triad of podia in ambulacrum III and the dental sacs in interambulacra 2 and 3 (Fig. 8, 10). Thus, *P. japonica* appears to conserve traits of indirect-developing sand dollars, except for adult rudiment location.

Kitazawa et al. (2004) discovered two asymmetric traits along the left-right axis in *P. japonica* larvae: shifts toward the left dorsal side of both the vestibular opening and the ciliary band. Together with subsequent enlargement of the vestibular opening and dorsal expansion of the oral field, Kitazawa et al. (2004) observed part of the adult rudiment, such as the podia, through the vestibular opening by scanning electron microscopy. This external observation is consistent with our internal observations that there is a leftward tilt of the left somatocoel encircling the hydrocoel and a concomitant leftward shift of the primary lobe (Fig. 8, 10). These observations indicate that *P. japonica* retains ancestral asymmetry along the left-right axis and furthermore that the location of the adult rudiment in *P. japonica* is not as exceptional as previously thought.

EXPERIMENTAL PROCEDURES

Animals, Embryos, and Larvae

Adult *P. japonica* were collected in Matsushima beach, Noto Island, Ishikawa, Japan.

Gametes were obtained by intracoelomic injection of 0.5 M KCl. Embryos, larvae, and juveniles were cultured in plastic dishes at 24°C in Marine Art SF-1 artificial seawater (Tomita Pharmaceutical, Tokushima, Japan). To culture juveniles, the seawater was changed every other day, and a new suspension of the diatom *Chaetoceros gracilis* was added.

Reconstruction of Three-dimensional (3D) Images

For anatomical observations, embryos and larvae were fixed with 4% paraformaldehyde in artificial seawater (van't Hoff, 1903), dehydrated in an ethanol series and acetone, embedded in Technovit 8100 (Heraeus Kulzur, Hanau, Germany), and cut serially into 2.5–3 µm thick sections on a microtome LEICA RM 2255 (Leica, Nussloch, Germany). Sections were observed with a fluorescence microscope BZ-9000 (KEYENCE, Osaka, Japan). Because *P. japonica* embryos and larvae emit autofluorescence, we recorded fluorescence images of unstained sections. To reconstruct 3D images, the fluorescence images were converted to black and white and false-colored by hand with Adobe Photoshop CS5 (Adobe systems inc.,

San Jose, CA). To examine the formation of coelomic compartments, the ectodermal layer, a mass of mesenchyme cells (the left coelom), and archenteron-derived epithelia were colored green, red, and yellow, respectively. In the coloring process, mesenchyme cells scattered in the blastocoel, including the blastocoelar and skeletogenic cells, were eliminated. Three-dimensional images were reconstructed from colored section images using DeltaViewer (DeltaViewer Project, <http://vivaldi.ics.nara-wu.ac.jp/~wada/Delta-Viewer/>).

ACKNOWLEDGMENTS

We want to thank especially Dr. Shonan Amemiya and Dr. Takuya Minokawa for their technical advice and valuable comments regarding this study. We thank Dr. Atsuko Yamazaki for helpful discussions. We also thank Dr. Daisuke Kurokawa, Dr. Akihito Omori, and Ms. Natsu Katayama for technical advice on the microtomy, and Dr. Yuichi Sasayama for allowing us to use the fluorescence microscope, BZ-9000.

We thank the reviewers and editor whose thoughtful suggestions helped us to improve the manuscript.

This study was supported by JSPS KAKENHI grant-in-aids to J.T. and M.Y.

REFERENCES

Amemiya S, Arakawa E. 1996. Variation of cleavage pattern permitting normal development in a sand dollar, *Peronella japonica*: comparison with other sand dollars. *Dev Genes Evol* 206:125–135.

Amemiya S, Emler RB. 1992. The development and larval form of an Echinothurioid Echinoid, *Asthenosoma ijimai*, Revisited. *Biol Bull* 182:15–30.

David B, Mooi R. 1998. Major events in the evolution of echinoderms viewed by the light of embryology. In: Mooi R, Telford M, editors. *Echinoderms*. San Francisco. Rotterdam: Balkema. p. 21–28.

Emler RB, McEdward LR, Strathmann R. 1987. Echinoderm larval ecology viewed from the egg. In: Jangoux M, Lawrence MJ, editors. *Echinoderm Studies 2*. Rotterdam: CRC Press. p. 55–136.

Emler RB. 1990. World patterns of developmental mode in echinoid echinoderms. In: Hoshi Y, Yamashita O, editors. *Advance in invertebrate reproduction Vol. 5*. Amsterdam: Elsevier Science. p. 329–335.

Fell HB. 1946. The embryology of the viviparous ophiuroid *Amphipholis squamata* Delle Chiaje. *Trans Roy Soc New Zealand* 75:419–464.

Ferkowicz MJ, Raff RA. 2001. Wnt gene expression in sea urchin development: Heterochronies associated with the evolution of developmental mode. *Evol Dev* 3:24–33.

Gordon I. 1929. Skeletal development in Arbacia, Echinarachnius and Leptasterias. *Phil Trans R Soc London Ser B* 217:289–334.

Hotchkiss FHC. 1995. Lovén's law and adult ray homologies in echinoids, ophiuroids, edrioasteroids, and an ophiocistoid (Echinodermata: Eleutherozoa). *Proc Biol Soc Wash* 108:401–435.

Iijima M, Ishizuka Y, Nakajima Y, Amemiya S, Minokawa T. 2009. Evolutionary modification of specification for the endomesoderm in the direct developing echinoid *Peronella japonica*: loss of the endomesoderm-inducing signal originating from micromeres. *Dev Genes Evol* 219:235–247.

Kitazawa C, Amemiya S. 1997. Evagination of the amniotic cavity in larvae derived from lithium-treated embryos of a direct developing echinoid, *Peronella japonica*. *J Exp Zool* 279:309–312.

Kitazawa C, Takai KK, Nakajima Y, Fujisawa H, Amemiya S. 2004. LiCl inhibits the establishment of left-right asymmetry in larvae of the direct-developing echinoid *Peronella japonica*. *J Exp Zool A Comp Exp Biol* 301:707–717.

Kubota H. 1988. Crinoidea. In: Dan K, Sekiguchi K, Ando H, Watanabe H, editors. Development of invertebrate. Tokyo: Baifukan. p. 332–338.

Lovén S. 1874. Études sur les échinodées. Kong Svenska Vetensk Akad Handl 11:1–91.

MacBride EW. 1903. The development of *Echinus esculentus*, together with some points on the development of *E. miliaris* and *E. acutus*. Phil Trans R Soc B 195:285–330.

Mortensen TH. 1921. Studies of the development and larval form of echinoderms. Copenhagen: GEC Gad. 261 p.

Okazaki K. 1975. Normal development to metamorphosis. In: Czihak G, editor. The sea urchin embryo. Berlin: Springer. p. 177–232.

Okazaki K, Dan K. 1954. the metamorphosis of partial larvae of *peronella japonica mortensen*, a sand dollar. Bio Bull 106:83–99.

Peterson KJ, Arenas-Mena C, Davidson EH. 2000. The A/P axis in echinoderm ontogeny and evolution: evidence from fossils and molecules. Evol Dev 2:93–101.

Raff RA. 1987. Constraint, flexibility, and phylogenetic history in the evolution of direct development in sea urchins. *Dev Biol* 119:6–19.

Schatt P, Féral JP. 1996. Completely direct development of *Abatus cordatus*, a brooding schizasterid (Echinodermata: Echinoidea) from Kerguelen, with description of perigastrulation, a hypothetical new mode of gastrulation. *Biol Bull* 190:24–44.

Smith A. 1984. Echinoid palaeobiology. London: George Allen & Unwin. 190 p.

Smith MM, Smith LC, Cameron RA, Urry LA. 2008. The larval stages of the sea urchin, *Strongylocentrotus purpuratus*. *J Morphol* 269:713–733.

Strathmann R. 1978. The evolution and loss of feeding larval strategies of marine invertebrates. *Evolution* 32:894–906.

van't Hoff JH. 1903. Physical chemistry in the service of the sciences. Chicago: University of Chicago Press. 126 p.

von Übisch L. 1913. Die entwicklung von *Strongylocentrotus lividus* (*Echinus microtuberculatus*, *Arbacia pustulosa*). *Z Wiss Zool* 106:409–448.

Wray GA, Raff RA. 1991. The evolution of developmental strategy in marine invertebrate. *Trends Ecol Evol* 6:45-50.

Yajima M. 2007. Evolutionary modification of mesenchyme cells in sand dollars in the transition from indirect to direct development. *Evol Dev* 9:257–266.

FIGURE LEGENDS

Fig. 1. Development of *P. japonica* (**A–F**) and schematic drawings of larvae (**G–I**; redrawn after Okazaki and Dan, 1954, Fig. 1). **A:** Embryo at the 16-cell stage (2.5 h, lateral view). Micromeres are formed at the vegetal pole. **B:** Blastula before hatching (9 h, lateral view). The primary mesenchyme cells ingress into the blastocoel. **C:** Gastrula (16 h, lateral view). Mesenchyme cells migrated out of the archenteron tip. **D:** Late gastrula (18 h, oral view). Stomodeum-like invagination in the oral field is vestibule. **E:** Early pluteus larva (24 h, dorsal view). Vestibule extends on the dorsal side of the larva. **F:** Juvenile after metamorphosis (4 days, aboral view). **G:** Prism larva (longitudinal section). **H:** Pluteus larva (longitudinal section). **I:** Pluteus larva (transverse section). A, anterior; P, posterior; D, dorsal; V, ventral; bp, blastopore; co, coelom; ec, enterocoelic sac; es, enteric sac; hy, hydrocoel; vc, vestibular cavity; ve, vestibule. Scale bar = 100 μm .

Fig. 2. Imago three weeks after metamorphosis fed with diatoms (aboral view). **A:** Bright field image. **B:** Fluorescence image. Green and red arrowheads indicate adult dental elements and anus, respectively. White and black arrowheads show remnant larval postoral rods, traces of the former anterior side of the larva. The digestive tract, fluorescing from chlorophyll, starts from the masticatory apparatus, involutes

twice, and ends at the anus between the postoral rods. This indicates that the anterioposterior axes of larvae and adults are parallel, but opposite in direction. Scale bar = 100 μm .

Fig. 3. Transverse sections of a gastrula at 16 h along the oral-aboral axis. **A:** Oral-side section. Vestibule invaginates in the oral field. **B:** Medial section. Archenteron leans toward the left side of the embryo. A number of mesenchyme cells have migrated out of the archenteron tip. Scale bar = 100 μm .

Fig. 4. Horizontal sections along the dorsoventral axis (**A–D**) and reconstructed three-dimensional images (**E–H**) of an early prism larva (18 h). (**A–D**) Four of 70 serial sections (3 μm thick) of the larva from the ventral bottom to dorsal top. The ectodermal layer, a mass of mesenchyme cells, and archenteron-derived epithelia are colored green, red, and yellow, respectively. Mesenchyme cells scattered in the blastocoel are eliminated. **A:** Ninth section from the ventral bottom (9/70). **B:** Fifteenth section (15/70). **C:** Twenty-fifth section (25/70). **D:** Thirty-fifth section (35/70). (**E–H**) Three-dimensional images reconstructed from serial sections using DeltaViewer, viewed from the right-posterior, slightly dorsal side of the larva. **E:** Exterior image with axial coordinates (A, anterior; P, posterior; D, dorsal; V, ventral; L, left; R, right). The image is shown in a reduced scale compared to those of internal structures (F–H). **F:**

Image of a mesenchymal mass. **G**: Image of whole endomesoderm. **H**: Image of archenteron-derived structures. Arrowheads (in D, G, and H) indicate the tip of the coelomic pouch adjacent to the vestibular floor. Asterisks (in C, G, and H) show portions where the boundary between the mesenchyme and enterocoelic epithelia is obscure. ar, archenteron; rc, right coelom. Scale bar = 100 μm .

Fig. 5. Horizontal sections along the dorsoventral axis of an early pluteus larva (24 h). (**A–F**) Six of 84 serial sections (3 μm thick) of the larva from the ventral bottom to dorsal top. The ectodermal layer, the left coelom developed from the mesenchyme plus an epithelial lobe, and archenteron-derived epithelia are colored green, red, and yellow, respectively. **A**: Sixth section from the ventral bottom (6/84). **B**: Ninth section (9/84). **C**: Thirteenth section (13/84). **D**: Twenty-third section (23/84). **E**: Twenty-eighth section (28/84). **F**: Thirty-second section (32/84). ar, archenteron; hy, hydrocoel; lc, left coelom; rc, right coelom; vf, vestibular floor. Scale bar = 100 μm .

Fig. 6. Three-dimensional images of an early pluteus larva (24 h) reconstructed from serial sections. (**A–D**) Images viewed from the right-posterior and slightly dorsal side of the larva. (**E–H**) Images viewed from left-anterior and slightly dorsal side. Color code is the same as in Fig. 5. The left coelom, marked in

red, expands to the anterior side of the larva on either side of the enterocoelic structures. The tip of the coelomic pouch elongates to the dorsal center of the larva to form the hydrocoel. Together with the original left side location, the C-shaped left coelom dominantly covers the enterocoelic structures on the left side. ar, archenteron; hy, hydrocoel; lc, left coelom; rc, right coelom.

Fig. 7. Horizontal sections along the dorsoventral axis of a pluteus larva (28 h). **(A–F)** Six of 65 serial sections (2.5 μm thick) of the larva from the ventral bottom to dorsal top. Color code is the same as in Fig. 5. **A:** Eleventh section from the ventral bottom (11/65). **B:** Nineteenth section (19/65). **C:** Twenty-fifth section (25/65). **D:** Twenty-eighth section (28/65). **E:** Thirty-fifth section (35/65). **F:** Fortieth section (40/65). hy, hydrocoel; lc, left coelom; rc, right coelom; vf, vestibular floor. Scale bar = 100 μm .

Fig. 8. Three-dimensional images of a pluteus larva (28 h) reconstructed from serial sections. **(A–D)** Images viewed from the right-posterior, slightly dorsal side of the larva. **(E–H)** Images viewed from left-anterior on the slightly dorsal side. Color code is the same as in Fig. 5. The formerly C-shaped left coelom has fused at the anterior side of the larva to encircle the hydrocoel, whereas the hydrocoel starts branching lobes in ambulacra II–IV. A triad of podia (blue asterisks) and radial canal develop exclusively

in ambulacrum III. I–V, ambulacra I–V; ds2, dental sac in interambulacrum 2; ds3, dental sac in interambulacrum 3; en, enteric sac; ra, radial canal; rc, right coelom.

Fig. 9. Horizontal sections along the dorsoventral axis of a pluteus larva (32 h). **(A–F)** Six of 71 serial sections (2.5 μm thick) of the larva from the ventral bottom to dorsal top. Color code is the same as in Fig. 5. **A:** Eighth section from the ventral bottom (8/71). **B:** Twelfth section (12/71). **C:** Sixteenth section (16/71). **D:** Twenty-third section (23/71). **E:** Thirtieth section (30/71). **F:** Thirty-third section (33/71). The right coelom, which has been largely segregated from the enteric sac (A–E), is narrowed in the anterodorsal portion (arrow in D) to divide it into the axocoel and right somatocoel. The axocoel is connected to the hydrocoel via a narrow duct (arrowhead in E). ac, axocoel; es, enteric sac; hy, hydrocoel; lsc, left somatocoel; rsc, right somatocoel; vf, vestibular floor. Scale bar = 100 μm .

Fig. 10. Three-dimensional images of a pluteus larva (32 h) reconstructed from serial sections. **(A–D)** Images viewed from the dorsal side of the larva. **(E–H)** Images viewed from the right-posterior and slightly dorsal side. Color code and axial coordinates are the same as in Fig. 5. The five lobes of the hydrocoel are evident, although closure of the hydrocoel crescent to form the ring canal has not yet

occurred between ambulacra IV and V (arrow in D). A podium primordia develops in ambulacrum II (arrowheads in D and H) along with a triad of podia in ambulacrum III (blue asterisks). Although the primary lobe is largely bilateral along Lovén's axis, it lies on the left side of the larva (C, D), together with a leftward tilt of left coelom (B, F). The left somatocoel has projected five dental sacs, which are interdigitated with five lobes (C, G). The axocoel is connected to the hydrocoel at the base of ambulacrum II via the stone canal. I–V, ambulacra I–V; ac, axocoel; ds1–5, dental sacs in interambulacra 1–5; en, enteric sac; ra2, 3, radial canal in amburaclum II, III; rsc, right somatocoel; st, stone canal.

Fig. S1. Original horizontal sections along the dorsoventral axis of an early prism larva (18 h). (A–P)

Sixteen serial sections (from the nineteenth to thirty fourth) of 70 serial sections (3 μm thick) of the larva from the ventral bottom to dorsal top. Arrowheads show an epithelial lobe projected posteriorly from the coelomic pouch. Scale bar = 25 μm .

Fig. S2. Original horizontal sections along the dorsoventral axis of an early pluteus larva (24 h). (A–P)

Sixteen serial sections (from the eleventh to twenty eighth) of 84 serial sections (3 μm thick) of the larva from the ventral bottom to dorsal top. Arrowheads show a part of the left coelom that developed probably by enterocoely from an epithelial lobe projected from the coelomic pouch at 18 h, whereas asterisks indicate coelomic cavities that formed probably by schizocoely in the mesenchyme. Scale bar = 25 μm .

Fig. 1

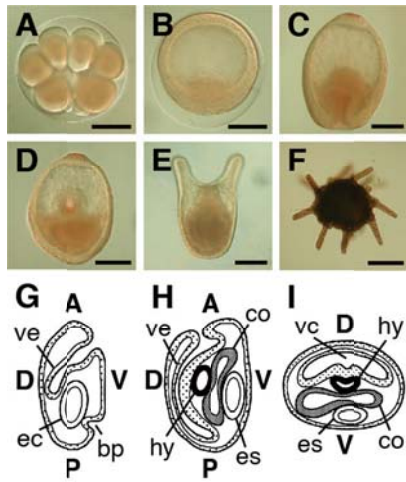


Fig. 2

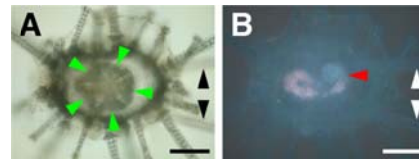


Fig. 3

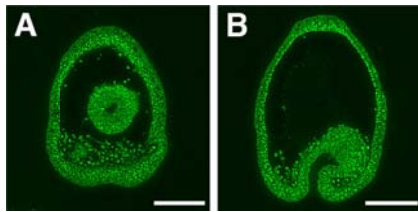


Fig. 4

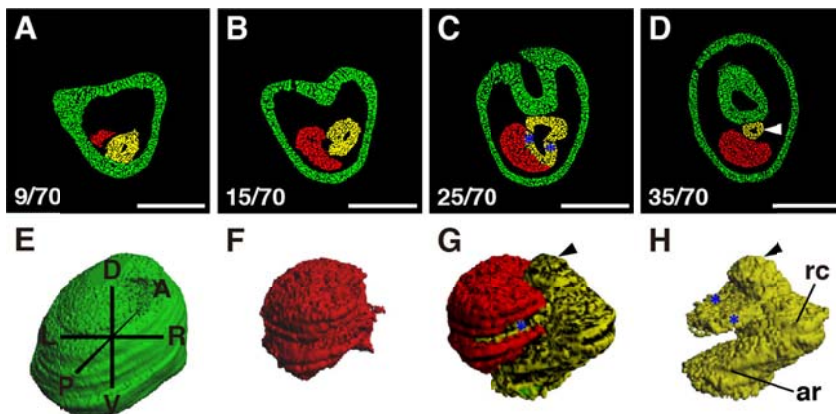


Fig. 5

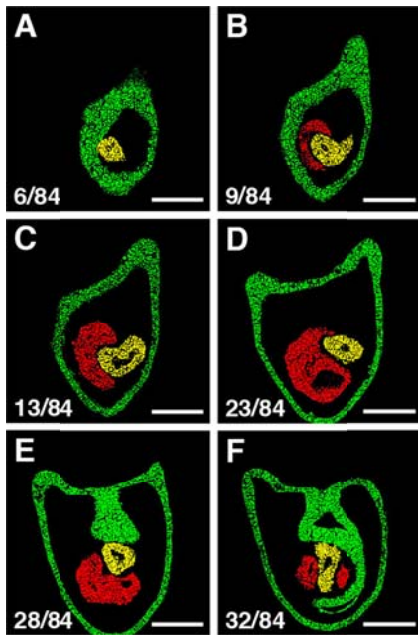


Fig. 7

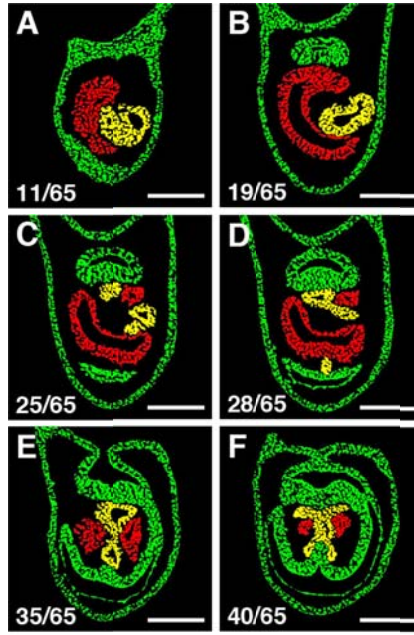


Fig. 6

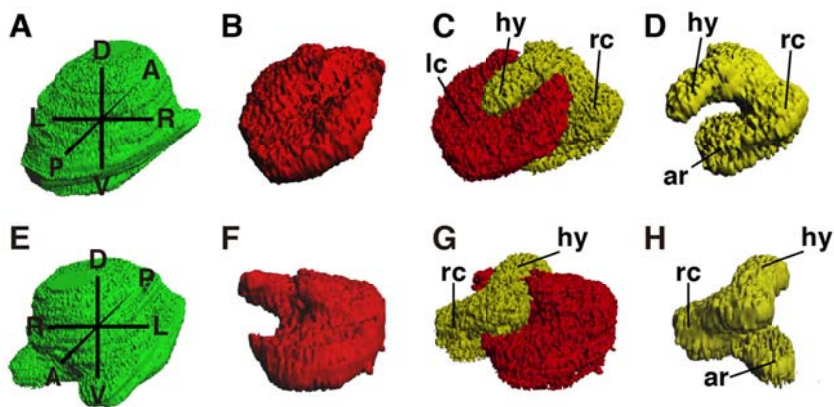


Fig. 8

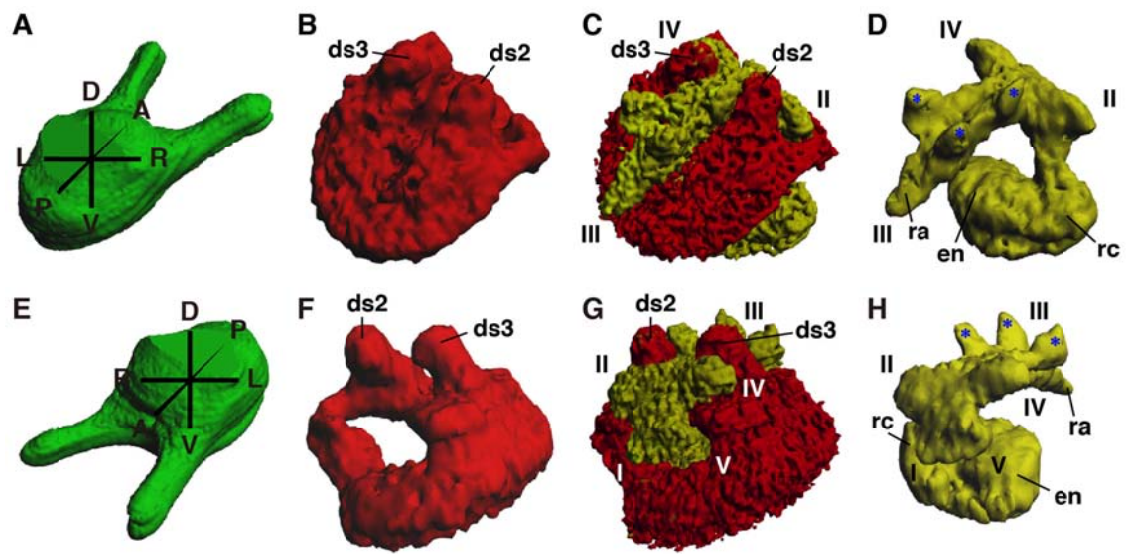


Fig. 9

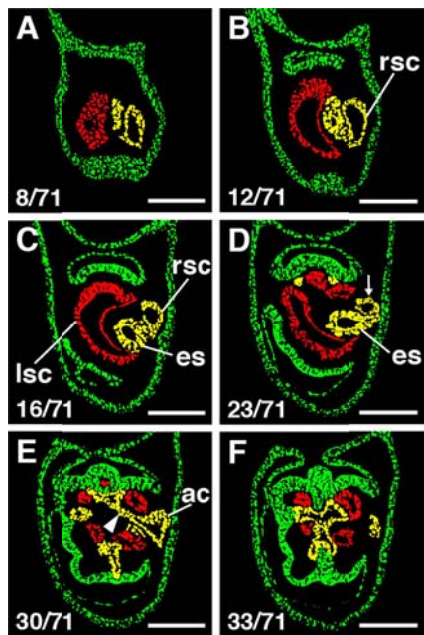


Fig. 10

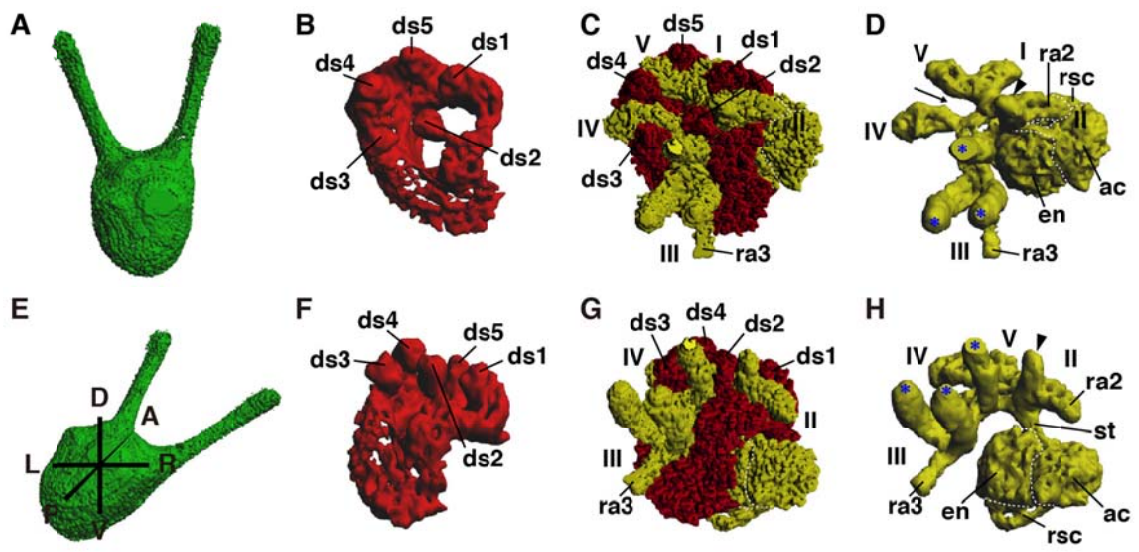


Fig. S1

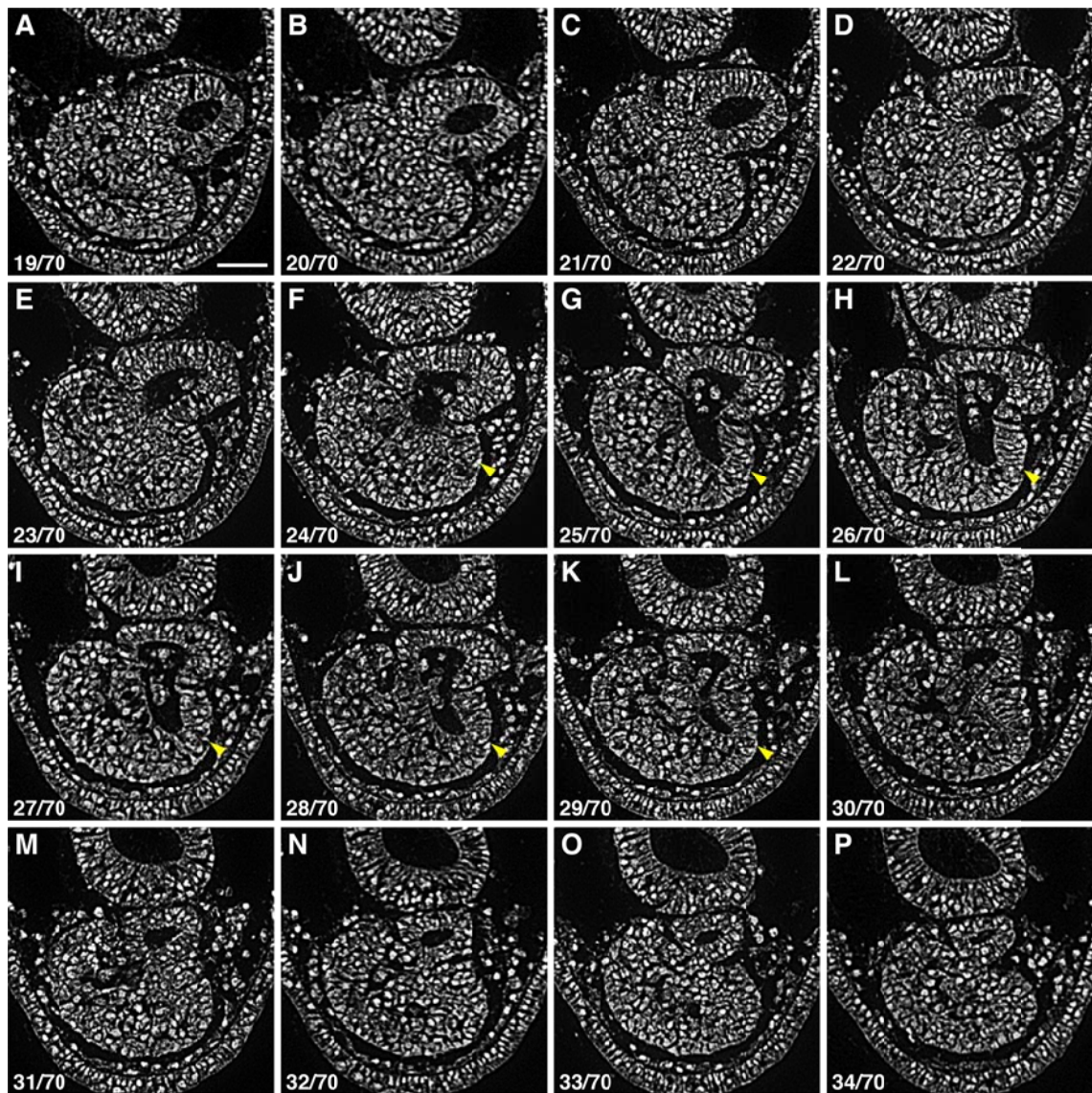


Fig. S2

